

Domain-Structured N¹,N²-Derivatized Hydrazines as Inhibitors of Ribonucleoside Diphosphate Reductase: Redox-Cycling Considerations

Shalom Sarel,*† C. Fizames,‡ Francois Lavelle,‡ and Shelly Avramovici-Grisaru†

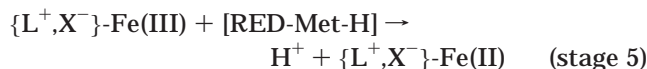
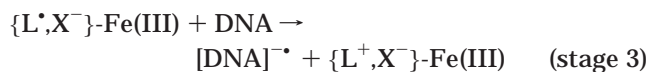
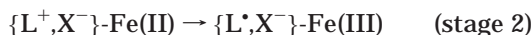
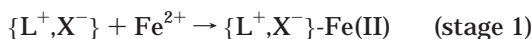
Department of Medicinal Chemistry, Hebrew University of Jerusalem, P.O. Box 12065, Jerusalem 91120, Israel, and Département Biologie, Service de Cancérologie, Rhône-Poulenc Rorer S.A., Centre de Recherches de Vitry-alfortville, 94403 Vitry-sur-Seine Cedex, France

Received July 6, 1998

Eight analogues of 1-[5-halogenosalicylidene]-2-[2'-pyridinoyl]hydrazine and -[2'-pyridyl]hydrazine, four of 1-[pyridoxylidene]-2-[2'-pyridinoyl]hydrazine, seven of 1-[pyridoxylidene]-2-[2'-pyridyl]hydrazine, and one each of 1,2-bis[pyridoxylidene]diaminoethane and bis[pyridoxylidenehydrazino]phthalazine were synthesized. Their solutions in DMF were assayed for activity against the metalloenzyme ribonucleoside diphosphate reductase (RdR), prepared from a subcutaneously growing murine tumor (sarcoma 180) implanted in B₆D₂F₃ male mice. The ¹⁴C-labeled CDP reductase was assayed by the modified method of Takeda and Weber, in which [¹⁴C]cytidine was separated from deoxycytidine by thin-layer chromatography (TLC) on cellulose foil. Distribution of radioactivity was assessed with an automatic TLC linear analyzer. Of the 31 compounds tested, 13 were essentially *inactive*, 7 were *highly active* against RdR, and the remaining 20 were slightly *more active* than hydroxyurea (used as a reference compound). The mechanism of inhibition is discussed in terms of three alternative pathways, initiated by sequestration of iron embedded in the R1 subunit of the metalloenzyme to form a C-centered chelate radical (via redox cycling). Alternatively, the latter could either reduce the tyrosyl radical or intercept radicals generated in the reduction process.

Introduction

1-[N-(Ethoxycarbonylmethyl)pyridoxylidonium]-2-[2'-pyridyl]hydrazine bromide (EPH) (16)^{1,2} represents a new class of orally active lipophilic chelators based on pyridoxal,^{3,4} which manifest a high affinity for iron and a high efficiency in removing toxic accumulations of iron in transfusional iron overload.^{1–5} Antimalarial *in vitro* studies have shown⁶ that in the absence of iron, EPH is essentially inactive against drug-resistant species of *Plasmodium falciparum* (FCR-3), the main causative agent of human malaria, whereas in the presence of Fe²⁺ ions, it appears to be highly active against FCR-3, with IC₅₀ = 1.9 μM. Moreover, whereas the EPH-Fe(III) chelate shows no activity against FCR-3, when living cells are absent, it exhibits high schizonticidal activity in the presence of living cells.⁷ These observations were rationalized⁸ in terms of a 5-stage *redox-cycling* process (stages 1–5), involving the intermediacy of a carbon-centered free radical {L[•],X⁻}-Fe(III) shown to function as the truly schizonticidal species responsible for the irreversible damage caused to cell DNA, as delineated below:



reductant-driven redox cycling of iron–chelate {L⁺,X⁻}-Fe(II) based on pyridoxal betaine

Corroboration of the above mechanism was forthcoming through: (i) UV spectroscopy [substantiating intramolecular electron transfer (stage 2)]; (ii) electron spin resonance (ESR), exhibiting signals at a_N = 15.75 G and a_H = 4.25 G (for PBN-R[•] spin adduct) (stage 3); and (iii) the nicks observed in the 43-kb linear double-strand of λ phage DNA and the nicks at bp 4363 in the supercoiled pBR322 plasmid DNA (stage 4). The regeneration of {L⁺,X⁻}-Fe(II) chelate, concurrently with the appearance of the {L[•],X⁻}-Fe(III) radical, from the corresponding Fe(III) chelate in the presence of living cells (possibly induced by cellular glutathione) (stage 5) became evident from ESR measurements.⁸

This development prompted a study aimed at establishing the ability of the redox cyclers EPH and analogues to inhibit the activity of ribonucleoside diphosphate reductase (RdR) (an iron-dependent metalloenzyme, constituting an *O*-tyrosine-centered radical⁹) which plays a pivotal role in DNA synthesis. Toward this end, we synthesized two classes of chelators: (i) one based on pyridoxal or on pyridoxal betaine (comprising 25 metal-free chelators and 6 metal chelates, see Charts 2–5) and (ii) one based on salicyl aldehyde (Chart 1). The 31 compounds included in this study were tested against RdR (prepared from a subcutaneously growing murine tumor—sarcoma 180—implanted in B₆D₂F₃ mice). The percent inhibition at various concentrations was evaluated relative to hydroxyurea. The results obtained are presented in Tables 1–5 and Figure 1.

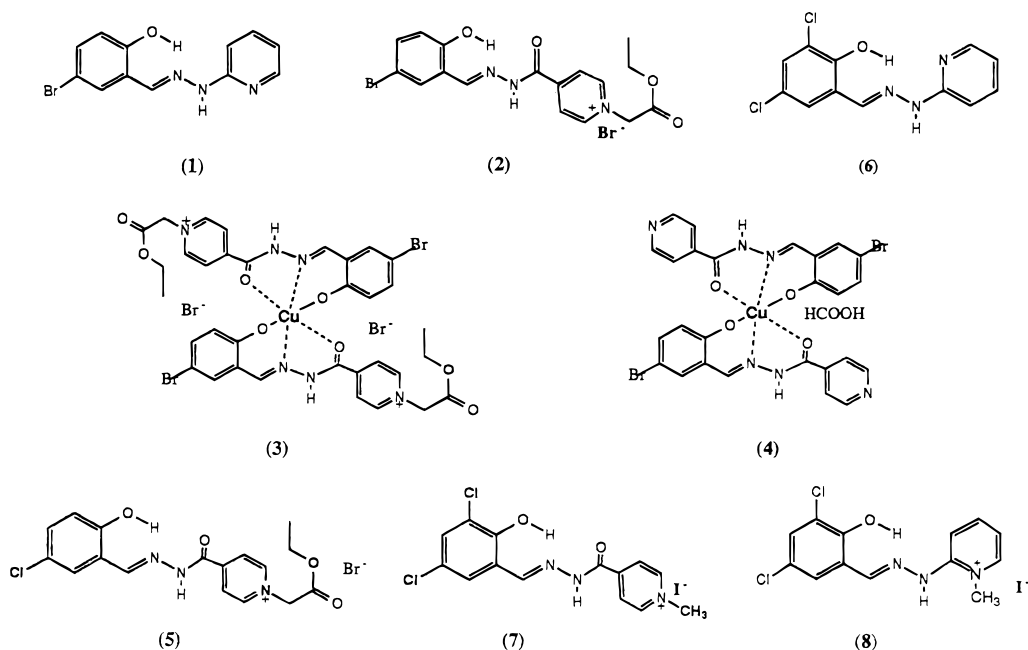
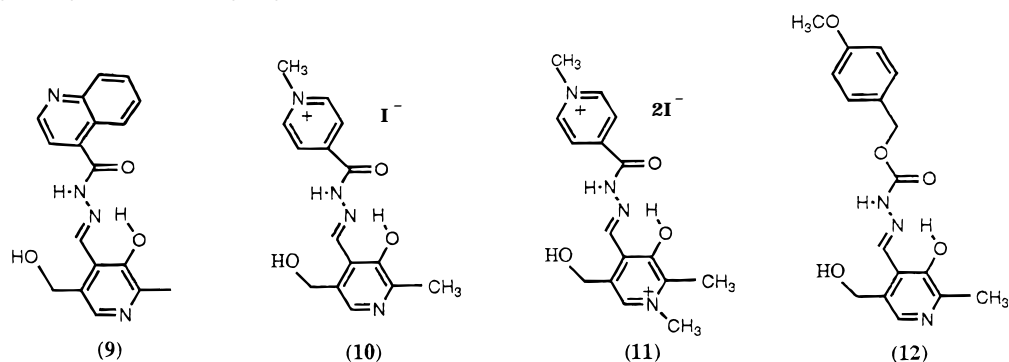
Results and Discussion

From Charts 1–5 it appears that, structurally, the chelators included in this study are made up of three distinctly different building blocks: (a) an *o*-hydroxy aromatic or heteroaromatic aldehyde (substituted salicyl

* To whom correspondence should be addressed. E-mail: sarel@cc.huji.ac.il.

† Hebrew University of Jerusalem.

‡ Rhône-Poulenc Rorer S.A.

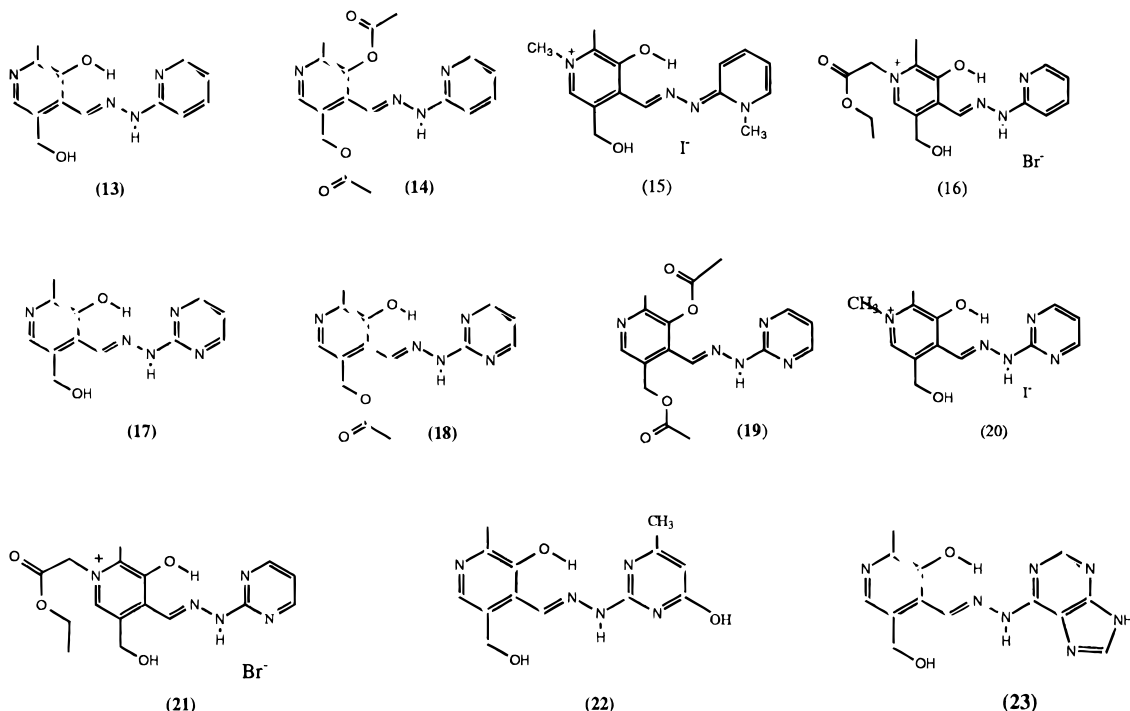
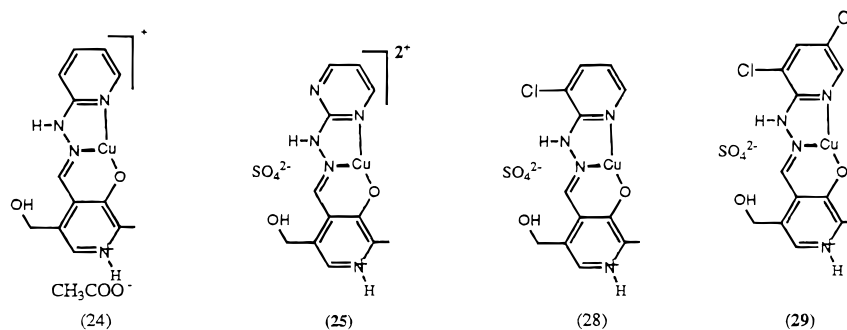
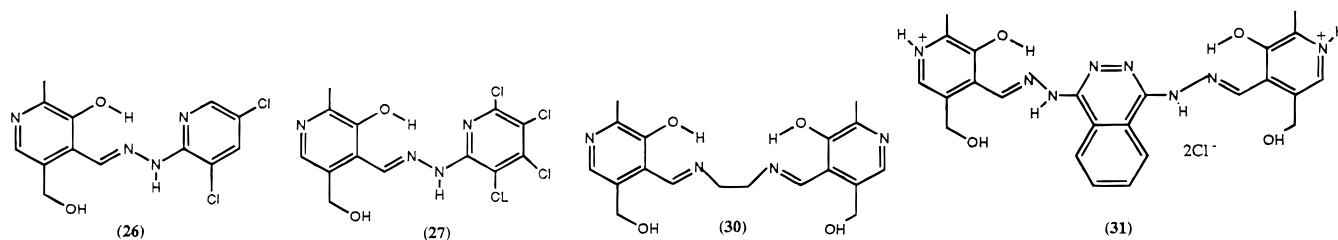
Chart 1. 1-[Halogenosalicylidene]-2-[aryl,aroyl]hydrazines**Chart 2.** 1-[Pyridoxylidene]-2-[aroyl]hydrazines

aldehyde or pyridoxal); (b) a heteroaromatic ring (pyridine, quinoline, pyrimidine, purine, or heteroaryl group (isonicotinoyl); and (c) an N^1, N^2 -disubstituted hydrazine (see Chart 5).¹⁴ The resulting hydrazones or aroyl hydrazones, contain inter-ring π -bridges of 4-atom chains, comprising two hydrazinic nitrogens of the $\text{CH}=\text{N}-\text{NH}^{\bullet}$ or $-\text{CH}=\text{N}-\text{NH}-\text{CO}$ type are capable of transmitting conjugative effects through the π -system. The chelators presented here constitute two distinctly different classes based on (i) chlorinated salicyl aldehyde (chelators **1–8**) and (ii) pyridoxal (**9, 10, 12–14, 17–19, 22–31**) or pyridoxal betaine (**11, 15, 16, 20–31**).

Class II is domain-structured,¹⁴ comprising four sites: (1) a metal-coordination site (O_2N), (2) a hydrophobic moiety (see Chart 6), (3) hydrogen-bonding sites (see Chart 6), and (iv) an electrophoric center. The latter constitutes a positively charged pyridinic ring N. Class I, by contrast, is devoid of two domains characteristic of class II, namely, the electrophoric and the hydrogen-bonding domains. The electrophoric site is distinctive in its ability to confer electron-sink properties upon the system,¹⁶ endowing the chelators with redox activity.⁷ Studies have shown that chelator **16** indeed functions as a reductant-driven redox cyler of iron (see Scheme 1).

The redox-active agents included here are potential inhibitors of RdR of the class I,^{9c–d} which is isolated from bacteria grown under aerobic conditions, including also mammalian and herpes simplex virus (HSV). The latter is composed of two homodimeric subunits, R1 and R2. R2 contains the cofactor, which is composed of an unusual μ -oxo-bridged diferric cluster adjacent to a tyrosyl radical (*Tyr122 in *Escherichia coli*).¹⁷ The tyrosyl radical is essential for catalysis and is generated by the diferrous form of R2 in the presence of O_2 .^{18,19} The X-ray structures of R1 and R2 from *E. coli*^{20,21} indicate that it contains binding sites for the purine and pyrimidine diphosphate substrates and for dNTPs and ATP, which act as allosteric effectors. The communication between R2 and R1 subunits, which are separated by ~ 35 Å, has been proposed to occur via a coupled electron- and proton-transfer process.²²

Mechanistically, the RdR inhibition may be conceived as arising either (i) from depriving the metalloenzyme of its iron cofactor,²³ (ii) by reduction of the tyrosyl radical into tyrosine, by transferring an electron to the O-centered radical (stage ii), or possibly (iii) by intercepting an intermediate radical generated in the process, as described below:

Chart 3. 1-[Pyridoxylidene]-2-[aryl]hydrazines**Chart 4.** Copper Chelates**Chart 5**

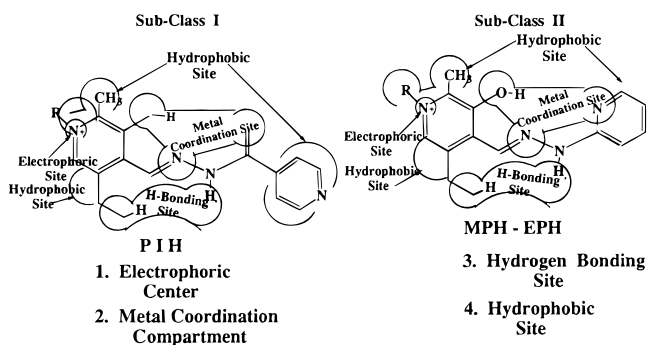
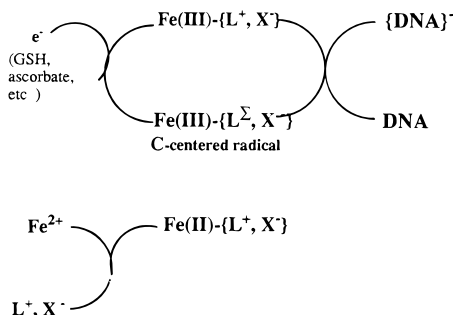
(i) RdR + ligand \rightarrow
apo-RdR (inactive) + Fe(III)-ligand

(ii) RdR-tyrosine-O⁺ + e⁻ \rightarrow
RdR-tyrosine-O⁻ (inactive)

(iii) {intermediate*} + Fe(III)-{L*,X⁻} \rightarrow
{intermediate*}-Fe(III)-{L,X⁻}

The data presented in Tables 1–4, and in Figure 1 relate to inhibition of RdR (from murine tumor-sarcoma 180) activity, by 31 different chelators described in the text. Of these 11 (**1**, **2**, **7**, **10–13**, **20**, **22**, **30**, and **31**), including analogues of PIH with high

avidity for iron, were essentially *inactive*. On the other hand, the pyridoxal pyridyl- and pyrimidinylhydrazones (**13**, **21**, and **26**), the salicylpyridyl hydrazones (**5** and **8**), and other analogues (**6**, **9**, and **23**) demonstrated the highest anti-RdR activity in reference to hydroxyurea (HU), by factors of 5.48, 4.8, and 3.8, respectively. The other six (**3**, **14**, **17**, **24**, **25**, and **29**) and five (**4**, **18**, **19**, **27**, and **28**) chelators were only moderately more active than HU, by factors of 2.68 and 1.88, correspondingly. Consistently, the most effective *in vivo* iron mobilizers—pyridoxal betaine pyrimidylhydrazone (**21**) and its analogue pyridoxal purinylhydrazone (**23**)—are indeed shown to be strong inhibitors of RdR. By contrast, pyridoxal betaine pyridylhydrazone (**16**), which pos-

Chart 6. Four Domains of Pyridoxal-Based Chelators**Scheme 1.** Reductant-Driven Redox Cycling of Iron**Table 1.** Inhibition of RdR by 1-[Mono- and Dihalogenosalicylidene]-2-[aryl, aryl]hydrazines

chelator no.	formula	molecular weight	concn (mM)	inhibition of RdR (%)	
				chela-tor	hydroxy-urea
1	$C_{12}H_{10}N_3OBr$	292	0.01	0	
2	$C_{17}H_{17}N_3O_4Br_2$	505	1.0	81	
			0.01	0	15
3	$C_{34}H_{134}N_6O_{11}Br_4S_{1/2}Cu$	1103.5	1.0	71	72
			0.1	64	15
4	$C_{27}H_{20}N_6O_6Br_2Cu$	749.5	1.0	59	73
			0.1	28	
5	$C_{12}H_{17}N_3O_4BrCl$	441.5	1.0	22	15
			0.02	77	
6	$C_{12}H_9N_3OCl_2$	282	0.002	10	
			0.0002	18	82
7	$C_{14}H_{12}N_3O_2Cl_2I$	452	1.0	65	
			0.033	34	
8	$C_{13}H_{12}N_3O_{1.5}Cl_2I$	432	0.00033	12	
			0.01	0	15
			0.033	58	82
			0.0033	34	
			0.00033	8	

esses high avidity for iron and also high tendency to enter into redox cycling, was essentially *inactive* against RdR. Noteworthy, the four strongest inhibitors of RdR, chelators **5**, **6**, **9**, and **26**, were also cytotoxic.

Of particular interest is the substitution effects presented here. Thus, replacing the pyridyl ring ($pK_a = 5.2$) in **13** by a 2-pyrimidinyl radical ($pK_a = 2.3^{25}$) (**13** \rightarrow **17**) decreased the anti-RdR activity by a factor of 2.79, but its activity increases by a factor of 1.88 on replacing the 2-pyrimidinyl by a 4-purinyl radical ($pK_a = 8.9^{26}$) (**17** \rightarrow **23**), and on **17** \rightarrow **21** conversion it increases by a factor of 2.63 (see Table 3 and Figure 1). The electronic effect of substitution is noticed on increasing the electron density on the pyrimidinyl ring (**17** \rightarrow **22**), rendering the chelator inactive toward RdR. In this context

Table 2. Inhibition of RdR by 1-[Pyridoxylidene]-2-[aroyl]hydrazines

chelator no.	formula	molecular weight	concn (mM)	inhibition of RdR (%)	
				chela-tor	hydroxy-urea
9	$C_{18}H_{17}N_4O_3Cl$	372.5	1.0		81
			0.027	63	
			0.0027	32	
			0.0002	11	
10	$C_{15}H_{17}N_4O_3I$	428	0.01	0	15
11	$C_{16}H_{20}N_4O_3I$	570	0.01	0	15
12	$C_{17}H_{18}N_5O_5$	344	0.01	0	15

Table 3. Inhibition of RdR by 1-[Pyridoxylidene]-2-[aryl]hydrazines

chelator no.	formula	molecular weight	concn (mM)	inhibition of RdR (%)	
				chela-tor	hydroxy-urea
13	$C_{13}H_{15}N_4O_2Cl$	294.5	0.077	72	15
14	$C_{17}H_{18}N_4O_4$	342	1.0	65	73
			0.1	68	37
15	$C_{15}H_{21}N_4O_3I$	432	1.0	31	15
			0.01	0	81
16	$C_{17}H_{20}N_4O_4Br$	423	0.01	0	15
			1.0	78	73
17	$C_{12}H_{13}N_5O_2$	259	0.1	40	37
			0.01	30	15
18	$C_{14}H_{15}N_5O_3$	301	1.0	84	73
			0.1	45	37
19	$C_{16}H_{17}N_5O_4$	343	0.01	27	15
			1.0	79	73
20	$C_{15}H_{19}N_4O_2I$	414	0.1	43	37
			0.01	24	15
21	$C_{16}H_{20}N_5O_4Br$	425	0.01	0	15
			1.0	79	72
22	$C_{13}H_{15}N_5O_3$	289	0.1	76	
			0.01	79	15
23	$C_{13}H_{13}N_7O_2$	299	0.033	72	
			0.0033	21	
			0.00033	18	

Table 4. Inhibition of RdR by Copper Chelates of Chelators **13**, **17**, and **26**

chelator no.	formula	molecular weight	concn (mM)	inhibition of RdR (%)	
				chela-tor	hydroxy-urea
24	$C_{13}H_{14}N_4O_6SCu$	417.5	1.0	90	73
			0.1	90	37
25	$C_{12}H_{17}N_5O_8SCu$	454.5	0.0	35	15
			1.0	86	73
28	$C_{13}H_{13}N_4O_6ClSCu$	452	0.1	78	37
			0.01	38	15
29	$C_{13}H_{12}N_4O_6Cl_2SCu$	486	1.0	82	81
			0.1	65	
			0.01	27	15
			1.0	85	81
			0.1	83	
			0.01	37	15

the effect of chlorination in **13** is of interest. Thus, whereas dichlorination of the pyridyl ring has no effect on its anti-RdR activity, tetrachlorination (**13** \rightarrow **27**) has a diminishing effect on its anti-RdR activity, by a factor of 3.18 (see Figure 1). It is not clear why N^1 -alkylation of **13** into **16** causes a loss of activity. The importance of H-bonding in the process is indicated in lowering the

Table 5. Inhibition of RdR by Some Pyridoxal Chloropyridyl Hydrazones, Dipyridoxals, Dihydrazones, and Diazines

chelator no.	formula	molecular weight	concn (mM)	inhibition of RdR (%)	
				chela- tor	hydroxy- urea
26	C ₁₃ H ₁₃ N ₄ O ₂ Cl ₃	362.5	1.0	83	72
			0.01	78	
			0.01	79	15
27	C ₁₃ H ₁₁ N ₄ O ₂ Cl ₅	432.5	1.0	43	72
			0.1	18	
			0.01	25	15
30	C ₁₈ H ₂₂ N ₄ O ₄	358	0.01	0	15
31	C ₂₄ H ₂₆ N ₈ O ₄ Cl ₂	561	0.01	0	15

activity on **17** → **18** and **17** → **19** acetylations, by 10% and 19%, respectively (Table 3). The effect of metal coordination is worthy of note. Whereas on **13** → **24** and **26** → **29** copper(II) sequestration the activity decreases, on **17** → **25** copper chelation the activity rather increases (see Table 4, Figure 1).

The mechanism of inhibition, as yet, is unknown. However, substitution effects presented here suggest that the active chelators are capable of binding to R1 (at sites for binding the purine and pyrimidine diphosphate substrates) and of extracting iron from the cofactor at R2; thus they effect the reduction of tyrosyl radical via reductant-driven redox cycling.^{7,8} Since the communication between R2 and R1 occurs via a coupled electron and proton process, it is also possible that an alternative mechanism is operating, which involves interception of intermediate radicals generated during the process. In view of the complexity of the enzymatic structure and mechanism of action, the tendency to redox cycle is certainly one factor, among others, which merits further study.

The information produced here is of particular significance for chelation therapy of transfusional iron overload.^{4,5} The observed inactivity of the orally effective chelator **16** toward RdR renders it a potential substitute for the naturally occurring desferrioxamine B (desferal), the only drug in current clinical use for removal of toxic surpluses of iron from the body.²⁷

Experimental Section

Materials. All the reagents and solvents were of "analytical" or "chemically pure" grades. Pyridoxal hydrochloride, mp 173 °C dec, was purchased from Merck. The following were purchased from Aldrich and used without further purification: 2,5-dichlorosalicyl aldehyde (mp 95–97 °C); 5-bromosalicyl aldehyde (mp 105–108°); 2-hydrazinopyridine (mp 45–46°); 1-[pyridoxylidene]-2-[2'-(4'-quinolinoyl)]hydrazine (mp 257 °C)³ (**9**); 1-[pyridoxylidene]-2-[*N*-methylisonicotinoyl]hydrazine iodide (mp 250 °C)^{1a} (**10**); 1-[*N*-methylpyridoxylidene]-2-[*N*-methylisonicotinoyl]hydrazine diiodide (mp 180 °C)¹¹ (**11**); 1-[pyridoxylidene]-2-[2'-pyridyl]hydrazine (mp 288 °C)¹² (**13**); 1-[*N*-methylpyridoxylidene]-2-[2'-*N*-methylpyridinium]hydrazine iodide (mp 276–277 °C)¹³ (**15**); 1-[*N*-(ethoxycarbonylmethyl)pyridoxylidene]-2-[2'-pyridyl]hydrazine bromide (mp 204 °C)² (**16**); 1-[pyridoxylidene]-2-[2'-pyrimidyl]hydrazine (mp 298 °C)¹⁴ (**17**); 1-[pyridoxylidene *O*²-acetate]-2-[2'-pyrimidyl]hydrazine (mp 177–178 °C)¹⁴ (**18**); 1-[*N*-methylpyridoxylidene]-2-[2'-pyrimidyl]hydrazine iodide (mp 252–3 °C)¹⁴ (**20**); 1-[*N*-(ethoxycarbonylmethyl)pyridoxylidene]-2-[2'-pyrimidyl]hydrazine bromide (mp 188 °C)¹⁴ (**21**); 1,4-[dipyridoxylidene]-1',2',3',4'-tetrahydrophthalazine (mp 275 °C)¹⁵ (**31**) were prepared as described.

1-[5'-Bromosalicylidene]-2-[2'-pyridyl]hydrazine (1). A solution of 2-hydrazinopyridine (1.1 g) in 1:3 acetic acid:water

(5 mL) was added dropwise with stirring at refluxing temperature to a solution of 5-bromosalicyl aldehyde (2 g) in 1:3 anhydrous CH₃COOH:H₂O (5 mL). A yellow precipitate was collected (95%) and recrystallized from ethanol, mp 221 °C.

1-[5'-Bromosalicylidene]-2-[*N*-(ethoxycarbonylmethyl)isonicotinoyl]hydrazine (2). A solution of 5-bromosalicyl aldehyde (2 g) in 1:3 anhydrous CH₃COOH:H₂O (5 mL) was added with stirring to a solution of *N*-(ethoxycarbonylmethyl)isonicotinoyl hydrazide (1.1 g) in 1:3 acetic acid:water (5 mL) at refluxing temperature. The resulting solid product (92%) was collected and recrystallized from ethanol, mp 265 °C. It gave the correct elemental analysis for C₁₇H₁₇N₃O₄Br₂.

1:2 Copper(II):1-[5'-Bromosalicylidene]-2-[*N*-(ethoxycarbonylmethyl)isonicotinoyl]hydrazine Sulfate Complex (3). An aqueous solution of CuSO₄·5H₂O (0.3 g, 1.25 mmol) in 5 mL of water was added at room temperature (rt) to a solution of 1-[5'-bromosalicylidene]-2-[*N*-(ethoxycarbonylmethyl)isonicotinoyl]hydrazine bromide (0.5 g, 1.25 mmol) in ethanol (25 mL), causing the pH to range between 3.0 and 4.0. A dark-brown precipitate (0.2 g, 42%) was collected and recrystallized from MeOH. IR (KBr, cm⁻¹): 1410, 1350s, 1290m, 1177vs, 1135vs, 1040w, 1010m, 975, 962w, 880, 855m, 810m, 750, 720, 700m, 675m, 640w, 550w, 505w, 460w, 326m. UV (MeOH): 427.7 nm (log ε 4.35), 341.5 (4.21), 338.6 (4.21), 246.0 (4.68), 229. (4.66), 201.3 (4.64).

1:2 Copper(II):1-[5'-Bromosalicylidene]-2-[isonicotinoyl]hydrazine Formate Complex (4). A solution of CuSO₄·5H₂O (0.25 g) in water (25 mL) was added with stirring to a solution of 5-bromosalicyl isonicotinoyl hydrazone (0.38 g, 1 mmol) in ethanol (25 mL) and refluxed for 30 min, causing the pH to range between 3.0 and 4.0. The solid green precipitate (340 mg, 90%) was collected and washed with methanol. UV (H₂O, c 5 × 10⁻⁶ M): λ_{max} 640 nm (log ε 1.80), 392.3 (3.89), 330.2 (3.86), 244.9 (4.22), 201.4 (4.01). IR (KBr, cm⁻¹): 3520–3350, 3250, 3060, 2960, 1600, 1495, 1455, 1415, 1352, 1320, 1300, 1245, 1210–1175, 1095, 1028, 945, 652, 812, 792, 750, 720, 640, 595, 550, 520, 465, 390, 332, 295.

1-[5'-Chlorosalicylidene]-2-[*N*-(ethoxycarbonylmethyl)isonicotinoyl]hydrazine (5). A solution of 5-chlorosalicyl aldehyde (0.2 g, 1 mmol) in ethanol (5 mL) was added to a solution of *N*-(ethoxycarbonylmethyl)isonicotinoyl hydrazide (224 mg, 1 mmol) in 5 mL of H₂O, and after briefly heating the resulting yellow precipitate (0.4 g) was collected. Recrystallization from methanol yielded crystals, mp 234 °C. They gave the correct elemental analysis for C₁₇H₁₇N₃O₄BrCl.

1-[3,5-Dichlorosalicylidene]-2-[2'-pyridyl]hydrazine (6). A solution of 2-hydrazinopyridine (115 mg, 1.1 mmol) was added with stirring under reflux, to a solution of 3,5-dichlorosalicyl aldehyde (191 mg, 1.1 mmol) in 1:3 anhydrous acetic acid:water (5 mL). After a few minutes of stirring, the light-yellow precipitate (275 mg, yield quantitative) was collected and recrystallized from methanol, mp 274–275 °C. UV (MeOH): λ_{max} 347.4 nm (log ε 4.34), 323 (4.24), 240.7 (4.28), 214.4 (4.27). IR (KBr, cm⁻¹): 3605, 3290, 3060, 2960, 2920, 2850, 1605, 1588, 1540, 1455, 1445, 1402, 1390, 1342, 1310, 1220, 1183, 900, 852, 851, 849, 843, 760, 733, 700. MS (EI) major peaks at *m/z*: 282 (M⁺), 280 (M – 2), 189 (M⁺ – C₅H₅N₂), 120 (C₆H₆N₃⁺), 67 (C₄H₅N⁺).

1-[3,5-Dichlorosalicylidene]-2-[*N*-methylisonicotinoyl]hydrazine Iodide (7). 1-[3,5-Dichlorosalicylidene]-2-[isonicotinoyl]hydrazone (450 mg, 1.5 mmol) was suspended in methyl iodide (5 mL) and refluxed for 24 h. After removal of MeI by distillation, the residue was recrystallized from ethanol.

1-[3,5-Dichlorosalicylidene]-2-[2'-*N*-methylpyridinium]hydrazine Iodide (8). A 400-mL volume of ethanol was added to a mixture of 1-[3,5-dichlorosalicylidene]-2-[2'-pyridyl]hydrazine (**6**) (2.82 g, 10 mmol) and MeI (3 g), and the mixture was refluxed for 48 h. The solvent and the unreacted reagent were removed by distillation, and the yellowish-brown solid residue was treated with boiling ethyl acetate, leaving behind 338 mg (8%) of the desired product (65% of the starting material was recovered as methiodide, mp 235 °C). Recrystallization from ethanol yielded semihydrated bright-yellow crystals, mp 251–

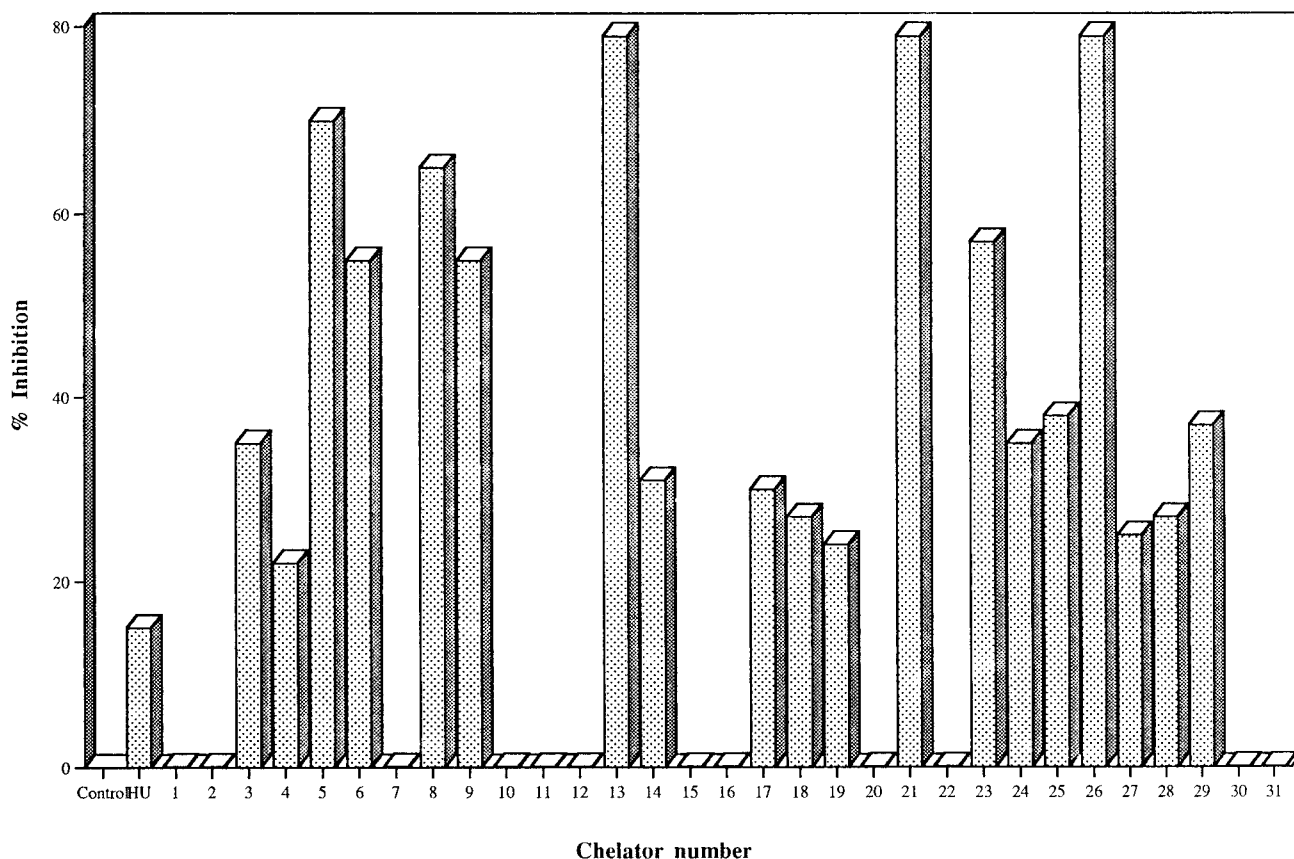


Figure 1. Percent inhibition of RdR by 10 mM chelator relative to 10 mM hydroxyurea (HU) in DMF solution.

252 °C. UV (MeOH): λ_{\max} 355.4 nm ($\log \epsilon$ 4.30), 351.4 (4.30), 339.6 (4.26), 305 (4.03), 219.9 (4.43). MS (EI) major peaks at m/z : 297 ($M^+ - I$), 295 ($M - 2H - I$), 278 ($M - H_2O - I$), 128 (HI^+).

1-[Pyridoxylidene O^1, O^2 -diacetate]-2-[2'-pyridyl]hydrazine (14). 1-[Pyridoxylidene]-2-[2'-pyridyl]hydrazine (0.5 g, 2 mmol), 9.4 mL of dry pyridine, and 15.6 mL of acetic anhydride were introduced into a flask well-protected from moisture. The mixture was briefly heated, and the solvent was removed by distillation in vacuo. The residue was extracted with ethyl acetate and treated with active charcoal. The solvent was partially evaporated, and the yellow crystals were collected, mp 209–210 °C. 1H NMR (300 MHz, Me_2SO-d_6): δ 11.74 (s, 1H), 11.48 (s, 1H), 8.40 (a, 2H), 8.23 (t, 1H, $J = 0.6$ Hz), 8.01 (s, 1H), 7.72 (t, 1H, $J = 0.6$ Hz), 6.93–6.80 (sept, 2H), 5.18 (s, 2H), 3.36 (s, 2H), 2.43 (s, 3H), 2.07 (s, 3H).

1-[Pyridoxylidene]-2-[4'-hydroxy-6'-methyl-2'-pyrimidyl]hydrazine (22). (a) **Hydrochloride.** A solution of 2-hydrazino-4-hydroxy-6-methylpyrimidine (0.14 g, 1 mmol) in 1:2 MeOH:H₂O (15 mL) was added to a stirred solution of pyridoxal hydrochloride (0.1, 1 mmol) in methanol (5 mL) at refluxing temperature for 30 min. On cooling the yellow crystals (2.7 g, 83%) were collected and recrystallized from 1:3 MeOH:H₂O, mp 290–291 °C (**22a**). MS (EI) (relative intensity) m/z : 289 (M^+ , 12), 165 ($C_8H_9N_2O_2^+$, 24), 140 ($C_7H_8N_2O_2^+$, 27), 126 ($C_8H_9NO_2^+$, 37), 125 ($C_8H_8N_2O_2^+$, 47), 109 (11), 98 (16).

(b) **Free Base.** The free base was obtained by exposing **22a** to the action of aqueous NH_4OH , affording orange-yellow crystals, mp 276–277 °C (**22**). Alternatively, **22** could be prepared by adding **22a** (2 g) to an aqueous solution of sodium carbonate (0.5 g in 5 mL of H₂O). MS (EI) (relative intensity) m/z : 289 (M^+ , 23), 165 ($C_8H_9N_2O_2^+$, 42), 139 ($C_7H_5N_2O_2^+$, 100), 125 ($C_8H_8N_2O_2^+$, 100), 109 (68), 98 (12).

1-[Pyridoxylidene]-2-[6'-purinyl]hydrazine (23). A solution of pyridoxal hydrochloride (0.9 g, 4.5 mmol) in 30 mL of water was added dropwise with stirring to a solution of 6-hydrazinopurine (0.67 g, 4.5 mmol) in 45 mL of water at rt. The yellow precipitate was collected and washed first with hot

MeOH and then with ether, yielding a pure product (1.26 g, 81%), mp > 300 °C. MS (EI) (relative intensity) m/z : 299 (M^+ , 30), 281 ($M - H_2O$), 268 ($M - CH_2OH$), 166 ($C_7H_8N_3O_2^+$), 150 ($C_5H_6N_6^+$, base peak, 100), 135 ($C_5H_5N_5^+$, 90), 121 ($C_5H_5N_4^+$, 85), 108 ($C_4H_4N_4^+$, 85).

Copper(II) Chelate of 1-[Pyridoxylidene]-2-[2'-pyridyl]hydrazine Sulfate (24). A solution of $CuSO_4 \cdot 5H_2O$ (0.85 g, 3.39 mmol) in water (5 mL) was added with stirring to a solution of 1-[pyridoxylidene]-2-[2'-pyridyl]hydrazine (2 g, 6.78 mmol) in water (5 mL). The reaction mixture became acidic (pH ~ 3) and green-black in color. It was boiled for 30 min, the dark-green precipitate (0.4 g, 59%) was collected, washed with water and ethanol, and dried. UV (MeOH, $c 1 \times 10^{-3}$ M): λ_{\max} 466.9 nm ($\log \epsilon$ 4.13), 409 (4.23), 338.4 (4.23), 238.2 (4.49). It analyzed as a $C_{13}H_{14}N_4O_6SCu$ compound.

Copper(II) Chelate of 1-[Pyridoxylidene]-2-[2'-pyrimidyl]hydrazine Sulfate (25). An aqueous solution of $CuSO_4 \cdot 5H_2O$ (0.25 g, in 5 mL H₂O) was added to an ethanolic solution of free base 1-[pyridoxylidene]-2-[2'-pyrimidyl]hydrazine (0.26 g, 1 mmol in 150 mL of EtOH), and the resulting dark-green acidic (pH ~ 5) mixture was refluxed for 30 min. The black precipitate (0.43 g, 94.5%) was collected, washed with MeOH, and dried. UV (MeOH, $c 1 \times 10^{-3}$ M): λ_{\max} 443.6 nm ($\log \epsilon$ 3.64), 409.9 (3.79), 341.1 (3.75), 331.3 (3.76), 242.4 (4.09), 209.5 (3.84). IR (KBr, cm^{-1}): 3520–2560, 2420–2340, 2120, 2050, 1550s, 1430vs, 1385sh, 1350w, 1318m, 1280w, 1210s, 1158, 1130, 1090, 1003, 1000, 906w, 842w, 795w, 775, 750, 650, 600, 520, 508, 465, 310.

1-[Pyridoxylidene]-2-[3',5'-dichloro-2'-pyridyl]hydrazine Hydrochloride (26). A solution of pyridoxal hydrochloride (1 g, 5 mmol) in 6:1 MeOH:H₂O (35 mL) was added to a stirred solution of 2-hydrazino-3,5-dichloropyridine (1.18 g, 5 mmol) in 25 mL of MeOH at refluxing temperature. The cooled reaction mixture was diluted with ether, and the yellow precipitate was collected, mp > 320 °C. IR (KBr, cm^{-1}): 3210s, 3030m, 2600, 2030–2000, 1950, 1900, 1800m, 1630s, 1570s, 1530m, 1470m, 1430s, 1380vs, 1345s, 1300s, 1260s, 1230s, 1185–1150, 1120, 1100m, 1050s, 1010s, 920m, 900m, 890m,

810s, 735w, 620s, 550m. MS (EI) (relative intensity) m/z : 328 ($M^+ + 1$), 326 ($M - 1$), 307, 273 ($M - H_2O - 2H$), 165 ($C_8H_9N_2O_2^+$, 90), 162 (95), 150 ($C_9H_8NO_2^+$, base peak, 100), 120.

1-[Pyridoxylidene]-2-[3',4',5',6'-tetrachloro-2'-pyridyl]-hydrazine Hydrochloride (27). A solution of 2-hydrazino-3,4,5,6-tetrachloropyridine (0.5 g, 2 mmol) in ethanol (10 mL) was added dropwise to a stirred solution of pyridoxal hydrochloride (0.4 g, 2 mmol) in EtOH (10 mL) for 2–3 h. The cream-colored precipitate (0.766 g, 90%) was collected and recrystallized from MeOH, mp > 300 °C. MS (EI) (relative intensity) m/z : 396 (M^+ , 40), 393, 377, 375, 362, 232 ($C_5H_2N_2Cl_4^+$, 50), 230 ($C_5N_2Cl_4^+$, 48), 165 ($C_8H_9N_2O_2^+$, base peak, 100), 151 ($C_5H_9N_2O^+$), 137, 120.

Copper(II) Chelate of 1-[Pyridoxylidene]-2-[5'-chloro-2'-pyridyl]hydrazine Sulfate (29). An aqueous solution of $CuSO_4 \cdot 5H_2O$ (0.25 g, in 5 mL H_2O) was added to an ethanolic solution of 1-[pyridoxylidene]-2-[5'-chloro-2'-pyrimidyl]hydrazine (0.26 g, 1 mmol in 150 mL of EtOH), and the resulting dark-green acidic (pH ~ 5) mixture was refluxed for 30 min. The black precipitate (0.43 g, 94.5%) was collected, washed with hot MeOH, and dried. It analyzed as a $C_{13}H_{13}N_4O_6Cl_5SCu$ compound.

Copper(II) Chelate of 1-[Pyridoxylidene]-2-[3',5'-dichloro-2'-pyridyl]hydrazine Sulfate (30, 30a). An aqueous solution of $CuSO_4 \cdot 5H_2O$ (0.25 g, in 5 mL of H_2O) was added to a refluxing solution of 1-[pyridoxylidene]-2-[3',5'-dichloro-2'-pyridyl]hydrazine (0.36 g) in H_2O (10 mL). After an additional reflux for 30 min, the dark-green reaction mixture became acidic (pH ~ 3–4). The major crop of brown-green precipitate (0.37 g, 80%) (30) was collected, washed with MeOH, and dried. The dark-green mother liquor was allowed to stand overnight, yielding a minor green precipitate (80 mg) (30a). Complex 30 exhibited UV bands (MeOH, $c 1 \times 10^{-3}$ M): λ_{max} 481.9 nm (log ϵ 3.86), 361.6 (3.67), 339.9 (3.53), 246.1 (3.91), 204.6 (3.90). IR (KBr , cm^{-1}): 3400–3340, 3150, 3060, 2900, 2840, 2780, 1610s, 1530, 1460, 1435m, 1400m, 1390m, 1384m, 1320m, 1245m, 1188w, 1115m, 1072m, 1025m, 895s, 820w, 775w, 752w, 725w, 705w, 615m, 555w.

Although the IR spectrum of 30a was identical with that of 30, its UV (MeOH, $c 1 \times 10^{-3}$ M) differed slightly, exhibiting bands at λ_{max} 482.1 nm (log ϵ 3.88), 431.2 (3.73), 360.9 (3.75), 339.8 (3.63), 247.3 (3.00), 204.1 (3.97).

Biological Assays. RdR was extracted from a subcutaneously growing murine solid tumor–sarcoma 180–implanted in $B_6D_2F_3$ male mice.

Animals and Tumors: Maintenance of tumor-bearing and normal animals and excision of tumors and livers were as reported by Weber.¹⁰

Materials: ^{14}C -Labeled CDP and ATP were purchased from Radiochemical Center, Arlington Heights, IL. All other reagents were of the highest available grade.

Assay of CDP Reductase Activity: The standard CDP reductase assay mixture contained ^{14}C -labeled CDP, 0.6 mM (2 mCi/mmol); ATP, 6 mM; Mg acetate, 12 mM; DTE, 10 mM; HEPES buffer, 33 mM, pH 7.5; $FeCl_3$, 50 μM ; and the enzyme sample in a final reaction volume of 150 μL . The reaction was initiated by the addition of enzyme sample and was carried out at 37 °C. Incubations were terminated after 0, 10, and 20 min by boiling for 4 min, water was added, and the denatured protein was removed by centrifugation. In the supernatant fluid cytidine was separated from deoxycytidine by thin-layer chromatography (TLC) on cellulose foil (Scheicher and Schuell, F 1440/LS 254, 20 \times 20 cm with luminescer) using ammonium acetate, 5 M, pH 9 (10 mL), saturated sodium tetraborate (40 mL), ethanol (90 mL), and EDTA, 0.5 M (500 μL), over a period of 4 h. Distribution of radioactivity was assessed with an automatic TLC linear analyzer. Protein was determined by a routine method^{10c} with bovine serum albumin as standard. The results obtained are presented in Tables 1–5, and graphically presented in Figure 1.

Acknowledgment. This work was done (partly) in the framework of CDR Program C-7160, Grant No.

DPE-5544-G-SS-7021-00, for which we (S.S. and S.A.-G.) are thankful.

References

- (1) (a) Sarel, S.; Avramovici-Grisaru, S.; Hershko, C.; Link, G.; Spira, D. European Patent No. 0315 434 A2, Feb. 11, 1988. (b) Bergeron, R. J.; Streiff, R. R.; Wiegand, J.; Vinson, J. R. T.; Luchetta, G.; Evans, K. M.; Peter, H.; Jenny, H. B. *Ann. N. Y. Acad. Sci.* **1990**, *612*, 351–360.
- (2) Dounge, P.; Sarel, S.; Wongvisetsirikul, N.; Avramovici-Grisaru, S. *J. Chem. Soc., Perkin Trans. 2* **1995**, 319–323.
- (3) Avramovici-Grisaru, S.; Sarel, S.; Link, G.; Hershko, C. *J. Med. Chem.* **1983**, *26*, 298–302.
- (4) Hershko, C.; Link, G.; Pinson, A.; Avramovici-Grisaru, S.; Sarel, S.; Peter, H. H.; Hider, R. C.; Grady, R. W. *Ann. N. Y. Acad. Sci.* **1990**, *612*, 378–393.
- (5) Piomelli, S. *Ann. N. Y. Acad. Sci.* **1990**, *612*, 311–314.
- (6) Iheanacho, E. N.; Sarel, S.; Samuni, A.; Avramovici-Grisaru, S.; Spira, D. T. *Trans. R. Soc. Trop. Med. Hyg.* **1990**, *84*, 213–216.
- (7) Iheanacho, E. N.; Sarel, S.; Samuni, A.; Avramovici-Grisaru, S.; Spira, D. T. *Free Radical Res. Commun.* **1991**, *15*, 1–10.
- (8) Iheanacho, E. N.; Sarel, S.; Samuni, A.; Avramovici-Grisaru, S.; Spira, D. T. *Free Radical Res. Commun.* **1991**, *11*, 307–315.
- (9) (a) Lammers, M.; Follmann, H. *Struct. Bond.* **1983**, *54*, 29–91. (b) Nordlund, P.; Sjöberg, B.-M.; Eklund, H. *Nature* **1990**, *345*, 593–598. (c) Stubbe, J. A. *Annu. Rev. Biochem.* **1989**, *58*, 257–285. (d) Stubbe, J. A.; van der Donk, W. A. *Chem. Biol.* **1995**, *2*, 793–801. (e) Schirmer, R. H.; Müller, J. G.; Krauth-Siegel, R. L. *Angew. Chem., Int. Ed. Engl.* **1995**, *34*, 141–154.
- (10) (a) Weber, G. *N. Engl. J. Med.* **1977**, *296*, 486, 541. (b) Takeda, E.; Weber, G. *Life Sci.* **1981**, *28*, 1007–1014. (c) Lowry, O. H.; Rosebrough, H. J.; Parr, A. L.; Randall, R. J. *J. Biol. Chem.* **1951**, *193*, 265–275.
- (11) Avramovici-Grisaru, S.; Sarel, S.; Cohen, S. *J. Chem. Soc., Chem. Commun.* **1986**, 47–49.
- (12) Avramovici-Grisaru, S.; Cohen, S.; Sarel, S. *Heterocycles* **1990**, *30*, 1079–1090.
- (13) Avramovici-Grisaru, S.; Sarel, S.; Cohen, S. *J. Org. Chem.* **1989**, *55*, 5236–5241.
- (14) Sarel, S.; Cohen, S.; Avramovici-Grisaru, S. *Heterocycles* **1998**, *49*, 393–404.
- (15) Sarel, S.; Avramovici-Grisaru, S.; Bauminger, E. R.; Felner, I.; Nowik, I.; Williams, R. J. P.; Hughes, N. P. *Inorg. Chem.* **1989**, *28*, 4183–4187.
- (16) (a) Ponka, P.; Borova, J.; Neuwirt, Fuchs, O.; Necas, O. *Biochim. Biophys. Acta* **1979**, *586*, 278. (b) Huang, A. R.; Ponka, P. *Biochim. Biophys. Acta* **1983**, *757*, 306.
- (17) Reichard, P.; Ehrenberg, A. *Science* **1983**, *221*, 514–519.
- (18) Fontecave, M.; Nordlund, P.; Eklund, H.; Reichard, P. *Adv. Enzymol. Relat. Areas Mol. Biol.* **1992**, *65*, 147–183.
- (19) Bollinger, J. M.; Edmonson, D. E.; Huynh, B. H.; Filley, J.; Norton, J. R.; Stubbe, J. *Science* **1991**, *253*, 292–298.
- (20) Uhlin, U.; Eklund, H. *Nature* **1994**, *370*, 533–539.
- (21) Nordlund, P.; Sjöberg, B.-M.; Eklund, H. *Nature* **1990**, *345*, 593–598.
- (22) Karlsson, M.; Sahlin, M.; Sjöberg, B.-M. *J. Biol. Chem.* **1992**, *267*, 12622–12626.
- (23) In vitro iron chelation can reversibly inhibit ribonucleotide reductase¹⁷ and produce a potent inhibition of DNA synthesis in a variety of cellular systems.²⁴ Ex vivo studies have shown direct inhibition of RdR, isolated from human lymphocytes, by desferrioxamine.^{24c} Nyholm and colleagues^{24d} observed that iron chelators cannot remove iron from the M2 subunit of the enzyme but rather can chelate the iron required for synthesis and regeneration of functional M2 units.
- (24) (a) Bergeron, J. B. *Trends Biochem. Sci.* **1986**, *11*, 133–135. (b) Cavanaugh, P. F.; Porter, C. W.; Tukalo, D.; Frankfurt, D. S.; Pavelic, Z. P.; Bergeron, R. J. *Cancer Res.* **1985**, *45*, 4754. (c) Oblender, M.; Carpentieri, U. *Anticancer Res.* **1990**, *10*, 123–128. (d) Nyholm, S.; Mann, G. J.; Johansson, A. G.; Bergeron, R. J.; Gräslund, A.; Thelander, L. *J. Biol. Chem.* **1993**, *268*, 26200–26205.
- (25) Brown, D. J. *The Pyrimidines*; Interscience Publisher: London, 1962.
- (26) Joule, J. A.; Smith, G. F. *Heterocyclic Chemistry*, 2nd ed.; van Nostrand Reinhold: U.K., 1978.
- (27) Martell, A. E.; Anderson, W. F.; Badman, D., Eds. *Development of Iron Chelators for Clinical Use*; Elsevier/North-Holland: Amsterdam, 1981.